

## Dynamics of Four Triple Systems

ANDREI TOKOVININ<sup>1</sup>

<sup>1</sup>*Cerro Tololo Inter-American Observatory — NSF's NOIRLab Casilla 603, La Serena, Chile*

### ABSTRACT

Orbital motions in four hierarchical stellar systems discovered by speckle interferometry are studied. Their inner orbits are relatively well constrained, while the long outer orbits are less certain. The eccentric and misaligned inner orbits in the early-type hierarchies  $\epsilon$  Cha (B9V, central star of the 5 Myr old association,  $P = 6.4$  yr,  $e = 0.73$ ), and I 385 (A0V,  $P \sim 300$  yr,  $e \sim 0.8$ ) suggest past dynamical interactions. Their nearly equal masses could be explained by a dynamical decay of a 2+2 quadruple progenitor consisting of four similar stars. However, there is no evidence of the associated recoil, so similar masses could be just a consequence of accretion from the same core. The other two hierarchies, HIP 32475 (F0IV, inner period 12.2 yr) and HIP 42910 (K7V, inner period 6.8 yr), have smaller masses and are double twins where both inner and outer mass ratios are close to one. A double twin could either result from a merger of one inner pair in a 2+2 quadruple or can be formed by a successive fragmentation followed by accretion.

*Keywords:* binaries:visual stars:multiple stars:individual

### 1. INTRODUCTION

Multiple stellar systems are very diverse, ranging from compact planar worlds, where three or four stars are tightly packed within 1 au, to wide systems of 0.1 pc scale, often found in non-hierarchical configurations; see Tokovinin (2021a) for a review. Hierarchies with separations of 1–100 au, in the middle of this range, are more typical. Their dynamics (periods, eccentricities, mutual orbit orientation) bears imprints of the formation processes. However, only for a tiny fraction of known triple systems the inner and outer orbits could be determined or constrained owing to long (centuries and millenia) outer periods and insufficient data. It is increasingly clear that hierarchies were formed via several different channels.

In this work, orbits are determined for four such systems (Table 1), continuing similar studies reported in (Tokovinin 2021b; Tokovinin & Latham 2020; Tokovinin 2018a; Tokovinin & Latham 2017). Inner pairs in these systems were discovered a decade ago by speckle interferometry, and the data accumulated to date allow calculation of the first inner orbits. The outer orbits are not yet fully covered. Two systems ( $\epsilon$  Cha and I 385) have simi-

lar components of early spectral type arranged in apparently non-hierarchical configurations. Their inner orbits have large eccentricities, suggesting that dynamical interactions played a major role. The other two triples contain solar-type stars and are double twins where a pair of similar low-mass stars orbits the primary component with mass comparable to the mass of the pair. Despite apparent similarity, the two double twins have very different dynamics: the first has quasi-circular and aligned orbits, while in the other the inner orbit is highly eccentric.

The input data and methods are briefly introduced in Section 2. Sections 3–5 are devoted to individual systems. Their possible formation scenarios are discussed in Section 6.

### 2. DATA AND METHODS

#### 2.1. Speckle Interferometry

In the hierarchies studied here inner subsystems have been discovered by speckle interferometry with the high-resolution camera (HRCam) working on the 4 m telescopes SOAR (Southern Astrophysical Research Telescope) and Blanco located in Chile. HRCam, in use since 2007, is based on the electron multiplication CCD detectors. The instrument, data processing,

**Table 1.** List of Multiple Systems

WDS	Name	HIP	HD	$V$	$\varpi^a$	$P_{\text{out}}$	$P_{\text{in}}$	Masses
(J2000)				(mag)	(mas)	(yr)	(yr)	( $M_{\odot}$ )
06467+0822	HDS 940 A,BC	32475	49015	7.04	13.75 G	80.3	12.2	1.40+(0.69+0.65)
08447–2126	HDS 1260 A,BC	42910	...	10.19	27.51 G	125	6.9	0.72+(0.37+0.36)
11596–7813	$\epsilon$ Cha	58484	104174	4.90	9.02 H	750:	6.4	(2.57+2.45)+2.54
17248–5913	I 385 AD,B	85216	157081	7.25	3.85 G	2000:	300:	(2.32+2.03)+1.99

<sup>a</sup> Parallax codes: G — Gaia DR3 (Gaia Collaboration et al. 2021), H — Hipparcos (van Leeuwen 2007).

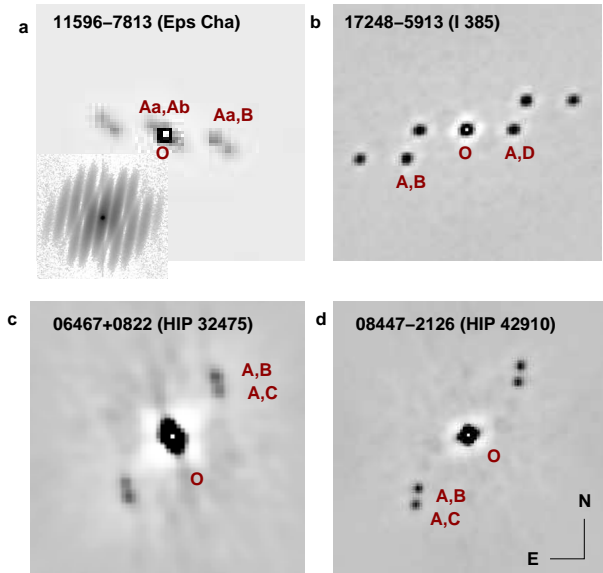


**Figure 1.** Speckle ACFs of triple stars recorded at SOAR (negative intensity rendering, standard orientation, arbitrary scale). In each panel, the white dot O marks the center, other labels indicate correct peaks corresponding to components’ pairs (other peaks are symmetric counterparts or complementary pairs). (a)  $\epsilon$  Cha on 2022.05, separations  $0''.054$  and  $0''.147$ ; insert shows the power spectrum. (b) I 385 on 2022.31, separations  $0''.29$  and  $0''.41$ . (c) 06478+0822 on 2022.77, separations  $0''.073$  and  $0''.34$ . (d) 08447–2126 on 2022.28, separations  $0''.067$  and  $0''.48$ .

and performance are covered in (Tokovinin et al. 2010; Tokovinin 2018b). The latest series of measurements and references to prior observations can be found in (Tokovinin et al. 2022). Image cubes of  $200 \times 200$  pixels and 400 frames are recorded mostly in the  $y$  (543/22 nm) and  $I$  (824/170 nm) filters with an exposure time of 25 ms or shorter and a pixel scale of 15 mas. In the  $y$  filter, the diffraction-limited resolution of 30 mas can be attained, and even closer separations can be measured via careful data modeling. On the other hand, the  $I$  filter offers deeper magnitude limit and better sensitivity to faint, red companions.

Image cubes are processed by the standard speckle method based on calculation of the spatial power spectrum and image auto-correlation function (ACF) derived from the latter. The  $180^\circ$  ambiguity of position angles inherent to this method is resolved by examination of the shift-and-add (“lucky”) images and by comparison with prior data. In a triple star, the angles of subsystems are related, so the better-defined orientation of the outer pair constrains the orientation of the inner subsystem. Figure 1 illustrates speckle data on the triple systems studied here. Recall that the positions and relative photometry are determined by modeling the power spectra, not by fitting the ACF peaks.

## 2.2. Orbit Calculation

As in the previous papers, an IDL code that fits simultaneously inner and outer orbits in a triple system has been used (Tokovinin 2017).<sup>1</sup> The method is presented in Tokovinin & Latham (2017). No useful radial velocity measurements are available for the systems studied here, so only positional measurements are used. The weights are inversely proportional to the squares of adopted measurement errors which range from 2 mas to  $0''.05$  and more (see Tokovinin 2021b, for further discussion of weighting).

Motion in a triple system can be described by two Keplerian orbits only approximately, but the effects of mutual dynamics are too small to be detectable with the current data. The code fits 14 elements of both orbits and the additional parameter  $f$  – the wobble factor, ratio of the astrometric wobble axis to the full axis of the inner orbit. For resolved triples,  $f = q/(1+q)$ , where  $q$  is the inner mass ratio. When the inner subsystem is not resolved, measurements of the outer pair refer to the photo-center of the inner pair, and the wobble amplitude corresponds to a smaller factor  $f^* = q/(1+q) - r/(1+r)$ , where  $r$  is the flux ratio. The code `orbit4.pro` can accept a mixture of resolved and unresolved outer po-

<sup>1</sup> Codebase: <http://dx.doi.org/10.5281/zenodo.321854>

sitions; it adopts a fixed ratio  $f^*/f$ , specified for each system as input parameter.

For the two early-type outer pairs discovered visually, position measurements at SOAR are complemented by the historic micrometer and speckle data retrieved from the Washington Double Star (WDS) database (Mason et al. 2001) on my request. Although such data extend the time coverage to almost 200 yr (for  $\epsilon$  Cha), it is still too short for constraining outer periods of several centuries. To avoid the degeneracy of outer orbits, some elements are fixed to reasonable values that agree with the estimated masses. The resulting outer orbits are only representative; however, they are still useful for the assessment of mutual dynamics.

The elements of inner and outer orbits in the selected triple systems are given in Table 3 in standard notation. Given the uncertain nature of outer orbits, the formal errors of their elements are meaningless, so they are not provided. Individual positions and their residuals to orbits are listed in Table 2, available in full electronically. Compared to the published HRCam data, the positions are corrected for the small systematics determined in (Tokovinin et al. 2022) and, in a few cases, re-processed. The second column indicates the subsystem; for example, A,BC refers to the angle and separation between A and unresolved pair BC, while A,B refers to the position of resolved component B relative to A.

### 3. EPSILON CHAMAELEONTIS

The bright ( $V = 4.90$ ,  $K = 4.98$  mag) B9V star  $\epsilon$  Cha (HR 4583, HD 104174, HIP 58484, WDS J11596–7813) is the central star of the young ( $5 \pm 2$  Myr, Dickson-Vandervelde et al. 2021)  $\epsilon$  Cha association located at  $\sim 100$  pc average distance (Murphy et al. 2013). The star has been resolved in 1835.93 into a  $1''.6$  binary with comparably bright components by Herschel (1847) and designated as HJ 4486. Subsequent monitoring with visual micrometers revealed a slowly decreasing separation with little change in position angle. Speckle-interferometric and Hipparcos measurements in the 1990s documented a separation of  $\sim 0''.4$ .

The pair A,B was closing down and lacked recent measurements, so it was observed at SOAR in 2015.25 on request by Ross Gould (Tokovinin et al. 2016). Quite unexpectedly,  $\epsilon$  Cha was revealed as a tight triple consisting of similar stars (Figure 1a). The inner pair Aa,Ab with a separation of 51 mas was expected to have a short orbital period and, indeed, its fast orbital motion was

detected in the following years (Briceño & Tokovinin 2017). In 2022 Aa,Ab has completed one full revolution since its discovery, and its orbit with a period of 6.4 yr is determined here.

The fluxes of the three components of  $\epsilon$  Cha are similar, but not exactly equal, which helps to establish the orientation. As shown in Figure 1a, the ACF peak below B is slightly weaker than the peak of B itself, thus defining the orientation of Ab relative to Aa as indicated. The 13 SOAR measurements in the  $y$  filter average to  $\Delta y_{Aa,Ab} = 0.25$  mag and have an rms scatter of 0.04 mag. At the same time,  $\Delta y_{Aa,B} = 0.11$  mag with a scatter of 0.07 mag. The combined magnitude of  $V = 4.90$  mag leads to the individual  $V$  magnitudes of Aa, Ab, and B: 5.98, 6.23, and 6.09 mag, respectively.

Speckle interferometry allows a position angle change by  $180^\circ$  (flip), but only simultaneous flips of both pairs in a triple are allowed. The orientation of A,B is defined by the historic measurements, thus fixing the angle of Aa,Ab. However, when in 2019 Aa,Ab closed down below the diffraction limit, the ACF peaks overlapped and it was no longer possible to discriminate reliably between opposite angles of the inner pair. The data of 2019 were originally processed under the assumption that Ab is located to the north of Aa, extrapolating its retrograde motion from the previous years. However, a negative  $\Delta y_{Aa,Ab}$  indicated that this assumption was incorrect, as also confirmed by the orbit. The SOAR observations in 2019 were re-fitted with the reversed orientation of Aa,Ab, which also affected the measured positions of Aa,B.

The orbits of Aa,Ab and A,B were fitted jointly. Apart from the WDS data, one speckle measurement made at Gemini-S in 2017.4 is used (Horch et al. 2019), the rest are SOAR measurements. The resulting wobble factor  $f = 0.48 \pm 0.02$  indicates that the masses of Aa and Ab are equal,  $q_{Aa,Ab} = 0.92 \pm 0.08$ . The first attempt to compute the orbit of Aa,Ab using wrong quadrants in 2019 resulted in an unrealistically small mass sum, but after quadrant correction the orbit of Aa,Ab becomes almost perfect (weighted rms residuals 0.9 mas) and corresponds to the inner mass sum of  $5.2 \pm 0.6 M_\odot$  using the Hipparcos parallax of 9.02 mas. The outer orbit, however, is not yet constrained by the observed arc, allowing a wide range of solutions. Two orbits of A,B are listed in Table 3: a circular one with  $P = 751$  yr and an eccentric orbit with  $P = 460$  yr. The circular orbit is adopted below; it corresponds to the mass sum of  $7.9 M_\odot$ . Dynamical stability of the triple system requires a separation of  $> 0''.2$  at the outer periastron, so the outer eccentricity should not exceed 0.8.

**Table 2.** Positional Measurements and Residuals

WDS	System	$T$	$\theta$	$\rho$	$\sigma$	$O-C_\theta$	$O-C_\rho$	Ref. <sup>a</sup>
		(yr)	( $^\circ$ )	( $''$ )	( $''$ )	( $^\circ$ )	( $''$ )	
06467+0822	B,C	2015.9063	2.6	0.0823	0.005	-1.0	0.0037	S
06467+0822	B,C	2015.9063	1.5	0.0835	0.005	-2.1	0.0049	S
06467+0822	B,C	2016.9575	33.5	0.0812	0.005	3.8	-0.0057	S

<sup>a</sup> H: Hipparcos; M: visual micrometer measurement; S: speckle interferometry at SOAR; s: speckle interferometry at other telescopes.

(This table is available in its entirety in machine-readable form)

**Table 3.** Orbital Elements

WDS	System	$P$	$T$	$e$	$a$	$\Omega$	$\omega$	$i$	$f$
		(yr)	(yr)		( $''$ )	( $^\circ$ )	( $^\circ$ )	( $^\circ$ )	
06467+0822	B,C	12.20	2011.70	0.095	0.0827	54.7	171.8	32.3	-0.50
		$\pm 0.38$	$\pm 0.06$	$\pm 0.032$	$\pm 0.0033$	$\pm 8.0$	$\pm 20.5$	$\pm 5.3$	$\pm 0.03$
06467+0822	A,BC	80.3	2029.0	0.072	0.382	23.6	324.7	30.7	...
		$\pm 1.9$	$\pm 5.7$	$\pm 0.055$	$\pm 0.108$	$\pm 7.5$	$\pm 20.0$	$\pm 5.7$	...
08447-2126	B,C	6.845	2016.416	0.948	0.0889	8.6	0	160.0	-0.48
		$\pm 0.034$	$\pm 0.023$	$\pm 0.006$	$\pm 0.009$	$\pm 0.6$	fixed	fixed	$\pm 0.03$
08447-2126	A,BC	125	2020.05	0.292	0.783	26.3	235.0	160.0	...
11596-7813	Aa,Ab	6.43	2018.57	0.733	0.0541	21.1	116.2	111.2	0.48
		$\pm 0.09$	$\pm 0.06$	$\pm 0.020$	$\pm 0.0022$	$\pm 1.5$	$\pm 2.2$	$\pm 1.8$	$\pm 0.02$
11596-7813	A,B	751	1837.4	0.0	1.481	181.4	0	83.5	...
11596-7813	A,B	460	2061.3	0.75	1.092	173.8	213.6	78.2	...
17248-5913	A,D	300	1969.0	0.80	0.280	271.5	242.0	90.0	0.43
17248-5913	AD,B	2000	1566	0.12	1.13	243.6	12.1	111.0	...

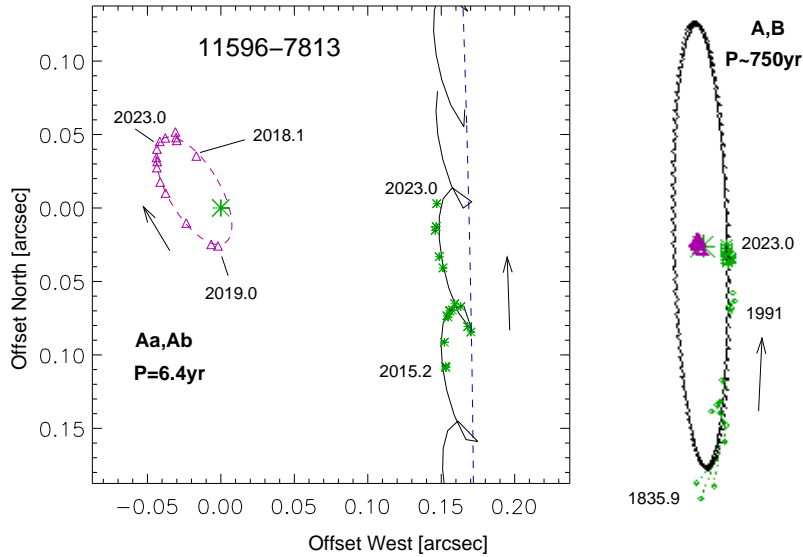


**Figure 2.** Orbits of  $\epsilon$  Cha. The right-hand plot shows the full circular outer orbit (crosses denote the less accurate micrometer measurements, squares show the resolved speckle data). The left-hand plot shows SOAR measurements of the inner pair (magenta ellipse and triangles) and the wavy line of the Aa,B motion with the superimposed wobble. The blue dashed line shows outer orbit without wobble.

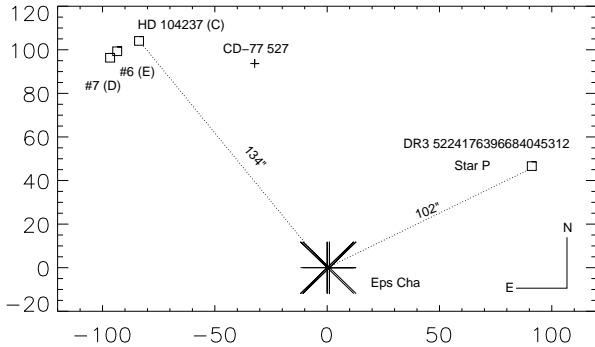


**Figure 3.** Closest neighbors of  $\epsilon$  Cha (axis scale in arcseconds) in Gaia DR3.

Note that the inner pair moves clockwise, the outer pair counterclockwise, so the two orbits cannot be coplanar. However, without identification of the correct ascending nodes of both orbits, the mutual inclination can take two possible values,  $156^\circ$  or  $34^\circ$  for the circular outer orbit ( $156^\circ$  and  $41^\circ$  for the eccentric one). The first value corresponds to counter-aligned orbital angular momenta, while the second implies only a modest inclination. It is likely that mutual inclination and inner eccentricity vary in Lidov-Kozai cycles. The large inner (and possibly outer) eccentricities attest, indirectly, to dynamical interaction between the orbits.

The Multiple Star Catalog (Tokovinin 2018c) and the WDS associate  $\epsilon$  Cha with another multiple system, HD 104237 (HIP 58520, DX Cha,  $V = 6.60$  mag, A7Ve) located at an angular distance of  $134''$  (projected separation 15 kau or 0.07 pc; FGL 1 AB,C). The projected separation implies an orbital period of  $\sim 0.5$  Myr if these stars are gravitationally bound. HD 104237 is a spectroscopic binary with a period of 19.86 days that has been extensively studied; it is accreting from a circumbinary disk (Dunhill et al. 2015). Furthermore, HD 104237 is surrounded by a swarm of five faint low-mass stars within  $15''$  according to Grady et al. (2004) and Gaia; the WDS code of this system is J12001-7812. I looked for objects within  $3'$  radius of  $\epsilon$  Cha in Gaia DR3 (Gaia Collaboration et al. 2021) and found another association member, DR3 5224176396684045312 ( $G = 15.23$  mag, parallax  $9.413 \pm 0.025$  mas, proper motion  $(-38.95, -5.48)$  mas yr $^{-1}$ ) at a distance of  $101''$ , denoted provisionally as star P. Location of the neighbors on the sky is illustrated in Figure 3. The star CD-77 527 situated between  $\epsilon$  Cha and HD 104237 does not belong to the association (parallax 3.44 mas).

Gaia does not provide parallax of  $\epsilon$  Cha, while Hipparcos measured  $9.02 \pm 0.36$  mas (new reduction, van Leeuwen 2007,  $8.95 \pm 0.58$  mas in the original catalog). Comparison of the Gaia and Hipparcos posi-

**Table 4.** Neighbors of  $\epsilon$  Cha in Gaia DR3

Name	Sep.	$G$	$\varpi$	$\mu_\alpha^*$	$\mu_\delta$	RUWE
	(arcsec)	(mag)	(mas)	(mas yr $^{-1}$ )		
$\epsilon$ Cha (AB)	0	4.78	9.02:	-42.9	-10.1	...
Star P	101.9	15.23	9.413	-39.0	-5.5	1.1
HD 104237 (C)	133.9	6.56	9.380	-39.3	-5.8	2.1
Eps Cha#6 (E)	136.7	13.01	9.769	-38.7	-3.1	1.4
Eps Cha#7 (D)	136.8	12.78	9.980	-42.8	-4.2	1.6

tions gives the best estimate of the proper motion (PM),  $(-42.85, -10.14)$  mas yr $^{-1}$ . Orbital motion of B relative to A with a speed of  $12.8$  mas yr $^{-1}$  is directed to the north. However, for multiples with equal components the centers of mass and light coincide ( $f^* = 0$ ), so correction of the PM for the orbital motion is not needed. Gaia DR3 measured a parallax of  $9.38 \pm 0.05$  for HD 104237, compatible within errors with the Hipparcos parallax of  $\epsilon$  Cha. The formal errors of Gaia and Hipparcos parallaxes cannot be fully trusted because astrometry of unresolved multiple systems is often biased. Table 4 lists parallaxes and PMs of the neighbors found in Gaia. Capital letters correspond to the components' designations in the WDS and MSC. The last column gives the Reduced Unit Weight Error (RUWE) as an indicator of the Gaia astrometric quality and potential subsystems. The closest satellite of HD 104237 at  $1''4$  separation (GRY 1 AF) has no parallax and PM in Gaia DR3, but the stability of its relative position over time proves that it is bound.

The projected separations of  $\epsilon$  Cha to its neighbors are within 15kau, typical for wide binaries and triples and suggesting that they may be bound. However, the PM differences of  $\sim 5$  mas yr $^{-1}$  ( $2.5$  km s $^{-1}$ ) in Table 4 appear highly significant. Note also that two satellites of HD 104237,  $\epsilon$  Cha #6 (E) and #7 (D) at  $10''$  and  $15''$  separations, respectively, have measurably different parallaxes, implying that this pair might be  $\sim 7$  pc closer to the Sun and simply projects onto HD 104237. So, the status of the neighbors remains undetermined. They could be either just independent members of the association or members of a bound (but likely dynamically unstable) stellar system.

The relative photometry of the  $\epsilon$  Cha components allows to place them on the color-magnitude diagram (CMD). The individual colors are not measured, but, given similar magnitudes, they should be close to the combined color  $V - K = -0.08$  mag. In Figure 4, the colors are arbitrarily offset from this value for il-

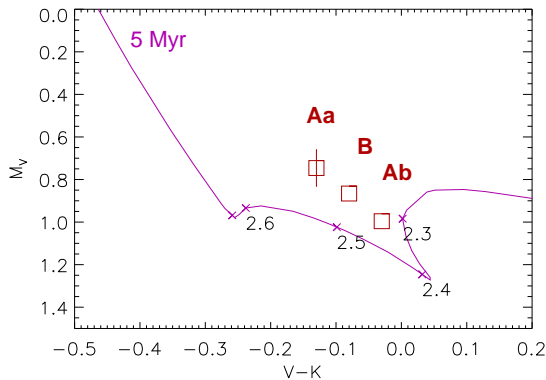


**Figure 4.** Location of  $\epsilon$  Cha components Aa, B, and Ab (red squares) on the  $(V, V - K)$  CMD. The error bar indicates the distance modulus uncertainty of  $\pm 0.08$  mag. The magenta curve is a 5 Myr PARSEC isochrone for solar metallicity (Bressan et al. 2012) with masses marked by asterisks and numbers.

illustration. Overall, the Hipparcos distance, inner orbit, and isochrone lead to consistent masses around  $2.5 M_{\odot}$ . However, the isochrone is not monotonous in this region, which is sometimes called H-peak (Guo et al. 2021) and corresponds to the ignition of hydrogen burning in young stars. At 5 Myr age, the H-peak is located at  $M_G$  between 0 and 1 mag, matching the absolute magnitudes of  $\epsilon$  Cha components. Given the uncertainties in the distance and color, potential inaccuracy of the isochrone, and its particular shape, it is hazardous to infer masses from the isochrone; the masses listed in Table 1 are tentative.

Considering the young age of  $\epsilon$  Cha and the continued accretion on its neighbor HD 104237, it was worth checking for the presence of hydrogen emissions in the spectrum. An optical echelle spectrum of  $\epsilon$  Cha has been taken on 2022 February 25 with the CHIRON echelle spectrometer on the 1.5-m telescope at Cerro Tololo (Tokovinin et al. 2013). The wide and deep hydrogen Balmer lines have no signs of emission, as established previously by Lyo et al. (2008). Apart from that, the spectrum is almost featureless. One notes only sharp telluric absorptions in the red part and a few very shallow and wide stellar lines. Thus, any residual gas around  $\epsilon$  Cha has been expelled and this system is not accreting at present. Its potential formation scenario is discussed below in Section 6.

#### 4. INNES 385

This remarkable quadruple stellar system is known as HIP 85216, HD 157081, WDS J17248–5913, and I 385. The bright visual triple consisting of the  $0''.5$  pair A,B with companion C at  $17''$  separation has been discovered by R. Innes in 1901 (Innes 1905); star C has similar PM

and parallax, hence it belongs to the system. Another star E listed in the WDS (28 $''$ 01, 109 $^{\circ}$ 3,  $G = 13.50$  mag) is optical, as evidenced by its distinct Gaia parallax (0.47 mas) and PM of  $(-0.4, -6.3)$  mas yr $^{-1}$ . The inner companion D, similar in brightness to A and B, has been discovered in 2008.5 by speckle interferometry (WSI 87 AD) at  $0''.26$  separation, while A,B was at  $0''.39$ , in a spectacular triangular configuration (Tokovinin et al. 2010) shown in Figure 1b. The object was regularly visited by the SOAR speckle camera since its discovery. During 14 years (2008.5 – 2022.3) the A,D pair has opened up slightly (from  $0''.26$  to  $0''.28$ ) at a rate of 2 mas yr $^{-1}$  with constant position angle, while A,B moved faster. A preliminary analysis of this system was provided in Tokovinin et al. (2016).

Examination of all available data has led to the firm conclusion that the speckle-interferometric observation of this star by the CHARA group in 1990.35 (Hartkopf et al. 1993) actually resolved the triple. Brian Mason consulted the archive and, indeed, the system was noted as having “possible third component”. The position of A,D was measured at  $270^{\circ}.2$  and  $0''.1994$ . This pre-discovery observation has not been published at the time, awaiting for a confirmation; it is used here. Curiously, the CHARA team also observed  $\epsilon$  Cha at a 4 m telescope in the 1990s three times, but they have not discovered the subsystem Aa,Ab.

Hipparcos measured the parallax of A as  $3.15 \pm 0.96$  mas (van Leeuwen 2007). Gaia does not give parallax of A because it is not a point source. However, the accurate Gaia DR3 parallax of star C ( $3.848 \pm 0.013$  mas) fixes the distance to this system. The Gaia astrometry of C is of good quality (RUWE=0.98). The PM of C,  $(-8.989, -11.557)$  mas yr $^{-1}$ , matches the Hipparcos PM of A,  $(-8.7, -14.5)$  mas yr $^{-1}$ ; however, the latter is a blend of A, B, and D biased by motion in the inner triple. The PM of A derived from its Hipparcos and Gaia positions is  $(-5.39, -12.26)$  mas yr $^{-1}$ .

The median magnitude differences of A with B and D in the  $y$  band are 0.49 and 0.42 mag, respectively (D is slightly brighter than B). Considering the combined magnitude  $V = 7.25$  mag, the individual  $V$  magnitudes of A, B, and D are 8.16, 8.65, 8.58 mag, respectively. The absolute magnitudes match main-sequence stars of masses 2.32, 1.99, and  $2.03 M_{\odot}$ , and the combined spectral type A0V corresponds to a star of  $2.3 M_{\odot}$ .

The fact that the inner, closer pair A,D moves slower than the wider pair A,B is unusual. Tokovinin et al. (2016) proposed two explanations. Star D could move on a wide orbit around A,B and project onto it. This configuration has a low probability and, moreover, the wide A,D orbit could be dynamically unstable with re-

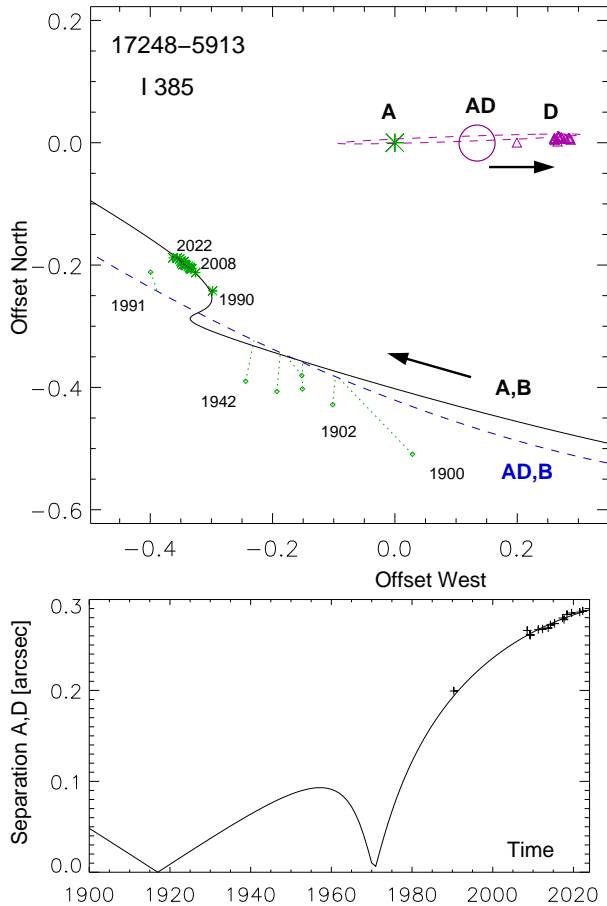


**Figure 5.** Orbital motion of the inner triple I 385. Top: motion of B relative to A (full line and green asterisks) or relative to the AD photo-center (blue dashed line and small diamonds). The magenta line and triangles show the orbit of A,D on the same scale. Star A is placed at the coordinate origin. The plot on the bottom shows angular separations of A,D vs. time. The inner pair was closer than  $0''.1$  throughout most of the 20th century and for this reason it has been missed by visual observers.

spect to the outer companion C. The other explanation of apparently slow A,D motion is because it is near apastron of an eccentric and highly inclined orbit. This more natural hypothesis is adopted and further explored here. The observations do not cover the long orbital periods of AD,B and A,D; the short observed segments can match a wide range of possible orbits. The question is whether some of those potential orbits are compatible with the distance and estimated masses. To answer it, just a pair of plausible orbits suffice.

First, I studied the motions of AD,B and A,D separately. A crude orbit of AD,B with  $P = 1244$  yr was suggested in (Tokovinin et al. 2016). I assume that the historic micrometer measurements of AD,B refer to the unresolved inner pair AD. The resolved speckle measure-

ments of A,B and A,D were transformed by replacing A with the average positions of A and D (center of mass), assuming that A and D are equal. After the initial fit, the elements  $P$  and  $a$  were fixed to the values that match the expected mass sum of  $6.3 M_{\odot}$ . The eccentricity of AD,B, essentially unconstrained, is fixed to a small value (a large eccentricity would render the inner pair dynamically unstable). The actual values of  $P, a$  can be substantially larger than those adopted here.

For the inner orbit of A,D, I adopted the period of 300 yr estimated from the projected separation, fixed  $e = 0.8$  and  $i = 90^{\circ}$ , and selected the element  $\omega$  to obtain the target mass sum of  $4.3 M_{\odot}$ . The resulting orbit fits well the observed slow motion of A,D. At present, the rate of its opening up decreases, and in several decades the pair will start to close down. In the final iteration, I used the `orbit4.pro` code to model both orbits simultaneously (see Table 3). The masses quoted above correspond to the wobble factor  $f = 0.47$ , while the fitted value is  $0.43 \pm 0.13$ . With the parallax of 3.85 mas, the inner and outer mass sums are  $4.4$  and  $6.3 M_{\odot}$  and, by design, match the photometric mass sums.

The orbits are illustrated in Figure 5. One notes that the first measurement of A,B by Innes in 1900 is inaccurate. Five micrometer measurements of AD,B in 1963–1979 are omitted, as well as the highly discrepant measurement by Innes in 1909.6 (discrepant micrometer measurements are common). The speckle measurement in 1990.35 by Hartkopf et al. (1993) at  $0''.384$  separation matches the resolved position of A,B rather than AD,B (indeed, the triple was resolved at the time but not announced), while the Hipparcos position in 1991.25 at  $0''.452$  better fits the unresolved pair AD,B; it was likely biased by the triple nature of the source. The tentative orbits demonstrate that the slow motion of A,D is compatible with an edge-on eccentric orbit. This orbit also explains why the triple has not been discovered earlier: throughout most of the 20th century A,D remained too close for a visual resolution.

## 5. DOUBLE TWINS HIP 32475 AND HIP 42910

The two triple systems featured in this Section have some common features. Both are double twins where a more massive primary star A is orbited by a twin secondary pair of low-mass stars B and C. The magnitude difference of B and C relative to A is substantial, about 3 mag, as in other similar double twins (Tokovinin 2018a). Yet another similarity are moderate ratios of the outer and inner periods.

The outer pairs in these two systems were discovered by Hipparcos and are named HDS 940 and HDS 1260, respectively, in the WDS. Both secondaries were re-

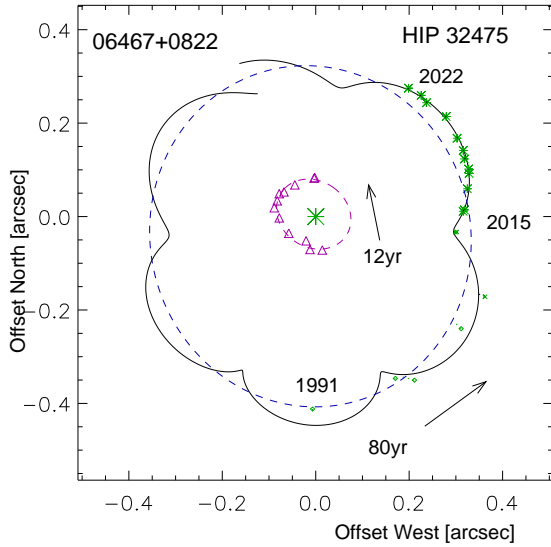


**Figure 6.** Orbits of HIP 32475 with periods of 12.2 yr and 80.3 yr. The blue dashed line marks the outer orbit without wobble that describes motion of BC around A, the black solid line is the motion of B relative to A. The orbit of B,C is plotted around coordinate origin on the same scale by the magenta line and triangles.

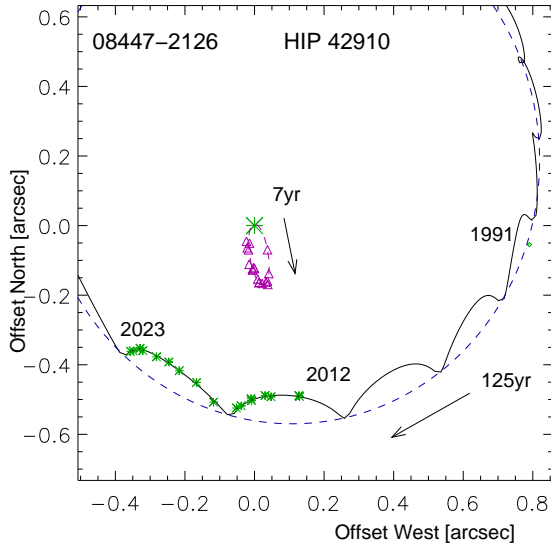


**Figure 7.** Orbits of HIP 42910; periods 6.8 yr and 125 yr.

solved into close pairs at SOAR in 2014 and 2015. Independently, Horch et al. (2017) discovered the triple nature of HIP 42910 in 2012. This team also observed HIP 32475 at the 3.5 m WIYN telescope five times from 1998 to 2012. They published only measurements of the outer pair A,BC and apparently missed the subsystem. Figure 1 shows typical speckle ACFs of these triples in the  $I$  band. Both systems are not resolved by Gaia. Orbital motion causes an increased astrometric noise and

potentially affects parallaxes, although the bias caused by the century-long outer orbits might be small.

The orbits are plotted in Figures 6 and 7 and their elements are given in Table 3. The positional measurements come from Hipparcos (outer pairs, epoch 1991.25), publications by Horch et al. (e.g. Horch et al. 2017), and SOAR. The coverage of both inner orbits is adequate, but the outer arcs are covered only partially. The shorter 80 yr outer orbit of HIP 32475 was determined by free fit, but for HIP 42910 the outer period and inclination were fixed. Preliminary orbits for this triple with periods of 106 and 9.06 yr were published by Horch et al. (2021); they disagree with all measurements available at present. A preliminary outer orbit of HIP 32475 with  $P = 128.9$  yr has been computed by Cvetković & Pavlović (2020).

The magnitude difference between components B and C of HIP 42910 is close to zero, so they can be swapped. An alternative to the eccentric inner orbit with  $P = 6.8$  yr could be a highly inclined near-circular orbit with approximately double period. A quasi-circular orbit was fitted to the measurements of B,C with suitably changed quadrants ( $P = 15.4$  yr,  $a = 0''.185$ ,  $e = 0.22$ ). However, its agreement with the measurements is worse, and the inner mass sum of  $1.28 M_{\odot}$  is much larger than allowed by the absolute magnitudes. So, the eccentric orbit of HIP 42910 B,C is the correct choice. However, the lack of measurements near its periastron, when the subsystem is below the SOAR resolution limit, does not fully constrain all elements. For this reason I fixed the inner elements  $\omega$  and  $i$  to the values that agree well with the data and lead to the expected inner mass sum of  $0.73 M_{\odot}$  (the free fit gives a slightly larger mass sum). The next inner periastron will occur in 2023.25, and the latest observation in 2023.0 confirms the decreasing separation.

Speckle interferometry at SOAR gives reliable measurements of the magnitude differences in the spectral band close to  $I$ . These data are assembled in Table 5. For HIP 32475, the combined  $I$  magnitude should be close to the  $G$ -band magnitude, 6.95 mag (the color indices are moderate). This assumption and the isochrones agree with the measured combined  $V$  and  $K$  magnitudes. For the redder star HIP 42910, I adopt the combined  $I = 8.70$  mag based on the following argument. After splitting the flux between components and deriving their absolute  $I$  magnitudes, I use the PARSEC isochrone (Bressan et al. 2012) for 1 Gyr and solar metallicity to estimate the masses and the combined  $V$  and  $K$  magnitudes of the system (10.10 and 7.10 mag,



**Table 5.** Photometry and Masses of HIP 32475 and 42910

HIP	Parameter	A+B+C	A-B	B-C	A	B	C
32475	$I$ (mag)	6.95	3.71	0.32	7.02	10.59	10.91
	$M$ ( $M_{\odot}$ )	...	...	...	1.40	0.69	0.65
42910	$I$ (mag)	8.70	2.97	0.06	8.83	11.80	11.86
	$M$ ( $M_{\odot}$ )	...	...	...	0.72	0.37	0.36

respectively). They are compared to the actually measured magnitudes (10.19 and 7.00 mag), and the best agreement is reached with the adopted combined  $I$ .

In HIP 32475, the main star A, of F0IV spectral type, is a  $\gamma$  Dor pulsating variable V830 Mon. Its photometrically estimated mass,  $1.40 M_{\odot}$ , is close to the estimated mass sum of the inner pair,  $1.34 M_{\odot}$ , so both inner and outer mass ratios are close to one (a double twin); the inner orbit and parallax give the mass sum of  $1.44 M_{\odot}$ . The inner mass ratio is directly measured by the wobble factor and, within errors, matches the photometric masses. The outer mass ratio can be checked by comparing the outer orbital motion with the proper motion anomaly, PMA (Brandt 2018). It equals  $(-10.7, -5.4)$  mas yr $^{-1}$  for the Gaia DR2 epoch of 2015.5, while the outer orbit predicts an effective motion of  $(+20.6, +11.1)$  mas yr $^{-1}$ . The ratio of PMA to orbital motion is close to  $-0.5$  and implies  $q_{A,BC} \approx 1$  if the photo-center motion is attributed to star A and the light of BC is neglected.

The estimated mass of HIP 42910 A,  $0.72 M_{\odot}$ , approximately matches its spectral type K7V. This is also a double twin. The inner orbit was tuned to obtain the expected mass sum of  $0.73 M_{\odot}$ , as noted above. The poorly constrained outer orbit yields a mass sum of  $1.45 M_{\odot}$ .

The similarity of those two hierarchies in terms of mass ratios and periods contrasts with very different character of their orbital motions. The orbits in HIP 32475 have moderate eccentricities and are oriented almost face-on. The most likely value of the mutual inclination is  $18^{\circ} \pm 6^{\circ}$  (the alternative value of  $60^{\circ}$  would have caused Lidov-Kozai cycles that would increase the inner eccentricity). The period ratio is small, 6.6, although it is not yet accurately known. Dynamical interactions in this low-hierarchy system are expected to be strong, and a mean motion resonance is possible. This triple system belongs to the family of “dancing twins” (Tokovinin 2018a). On the other hand, in HIP 42910 the inner orbit has a large eccentricity of 0.95, and the mutual inclination is either  $6^{\circ}$  or  $90^{\circ}$ .

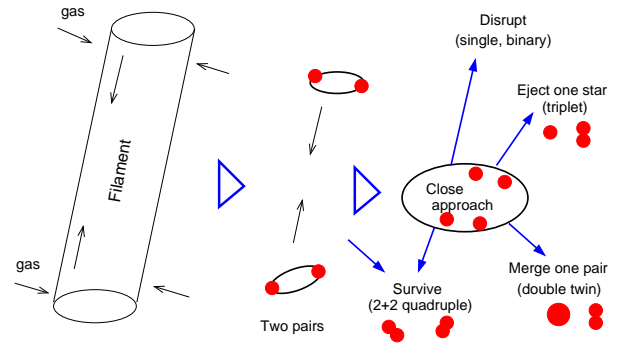


**Figure 8.** Possible scenario of forming hierarchical systems with comparable-mass components: triplets, quadruplets, and double twins.

It is firmly established that masses of stars in binaries are correlated instead of being chosen randomly (Duchêne & Kraus 2013; Moe & Di Stefano 2017). This trend extends to hierarchical systems. Quadruplets consisting of four similar stars arranged in 2+2 hierarchy stand apart as a distinct family of  $\epsilon$  Lyr type, although their orbital separations span a wide range (Tokovinin 2021a). Comparable masses are naturally explained by gas accretion onto a binary that tends to equalize masses and at the same time shrinks the orbits (Tokovinin & Moe 2020). Extension of this idea to triples helps to explain double twins where both inner and outer mass ratios are close to one (Tokovinin 2018a). However, existence of hierarchical systems of three similar stars (triplets) like  $\epsilon$  Cha with an outer mass ratio of 0.5 challenges the accretion scenario.

A possible path to form triplets is via dynamical decay of a 2+2 quadruple system. This scenario is illustrated in Figure 8. The initial condition is a filament of dense gas which grows by the accretion flow perpendicular to its axis. Inside the filament, the flow is directed along its axis. Two over-densities in the filament form two pairs of similar stars with orbits roughly perpendicular to the filament, owing to the angular momentum of the incoming gas. The total masses of both pairs are also comparable because they formed in the same filament and experienced comparable accretion rates. The pairs approach each other, driven by mutual attraction and by

## 6. DISCUSSION

the center-of-mass velocities inherited from the parental gas flow along the filament.

Close approach of two pairs and their dynamical interaction can lead to four different outcomes (Antognini & Thompson 2016). In the simplest case, the decay products are just single stars and binaries. If only one star is ejected, a bound triple with three similar components (a triplet) could result. Alternatively, one pair can become very close and merge, leaving a double twin. Finally, a bound 2+2 quadruple can emerge if the dynamical interaction was not too violent or did not happen at all. In all cases the surviving hierarchies bear imprints of chaotic dynamics, namely eccentric orbits with random mutual orientation.

The two massive triplets studied here ( $\epsilon$  Cha and I 385) match the proposed scenario: their inner orbits have large eccentricities and are not aligned with the outer orbits. HIP 42910, a double twin with eccentric inner orbit, could be a merger product. In contrast, the architecture of the double twin HIP 32475 with aligned quasi-circular orbits better matches the accretion scenario discussed in (Tokovinin 2018a).

A remarkable quadruple system FIN 332 (WDS J18455+0530, HIP 92027, HR 7048, the “tweedles”) illustrates the proposed scenario. It consists of four nearly equal A1V type stars in a 2+2 hierarchy (Tokovinin 2020). Orbits of the two inner twins have periods of 28 and 40 yr and large eccentricities (0.82 and 0.84); moreover, their apsidal axes point in approximately same direction. The outer pair ( $P \sim 5$  kyr) moves in the opposite sense and its orbit is definitely misaligned with orbits of the inner pairs. This architecture strongly suggests a past dynamical interaction. If one of the pairs in this system were disrupted and ejected a star, the result could resemble  $\epsilon$  Cha or I 385.

If  $\epsilon$  Cha is a product of a decaying 2+2 quadruple, one B-type star should have been ejected. Assuming an ejection speed of  $30 \text{ km s}^{-1}$ , the star would have traveled a  $\sim 150$  pc distance in 5 Myr. It is almost hopeless to search for the ejected star, it can be located anywhere on the sky. The phenomenon of runaway massive stars is well known, and it is generally accepted that many runaways were ejected from young unstable hierarchies (Hoogerwerf et al. 2000). For effective ejections, other members of these hierarchies must be also massive, and this consideration supports the dynamical scenario of forming massive triples and quadruples.

However, the scenario of triplet formation via decay of a 2+2 quadruple has a serious problem. Ejection of

one star with a velocity  $V$  causes recoil of the remaining triple with a velocity of  $\sim V/3$ . The facts that  $\epsilon$  Cha is close to the neighboring stars in the association and that I 385 is bound to another star C indicate absence of a fast recoil. Equal masses in triplets can be explained alternatively by accretion from a common gas reservoir while separations between the stars were still large and they moved randomly through the parental core without mutual dynamical interactions; otherwise, one star would have been ejected without a chance to grow further, as discussed by Reipurth (2000). The N-body dynamics may come into play later, when the system have migrated to a more compact configuration and the gas was mostly exhausted; the triple, nevertheless, avoids disruption and continues to move together with its neighbors.

Study of relative motions in hierarchical systems opens a fascinating window on their diversity and suggests formation via several channels, still poorly explored. Extension of such work to a much larger sample of hierarchies is highly desirable. However, long periods and the lack of historic measurements severely restrict potential samples. Indirect statistical approaches using only “instantaneous” data like positions and velocities (e.g. Hwang et al. 2022) are promising for the dynamical study of typical hierarchies with separations of 1–100 au. Long-term speckle monitoring of a large number of resolved hierarchies combined with precise Gaia astrometry will provide input data for these future investigations.

The research was funded by the NSF’s NOIRLab. I thank B. Mason for the analysis of archival observations of I 385. This work used the SIMBAD service operated by Centre des Données Stellaires (Strasbourg, France), bibliographic references from the Astrophysics Data System maintained by SAO/NASA, and the Washington Double Star Catalog maintained at USNO. This work has made use of data from the European Space Agency (ESA) mission *Gaia* (<https://www.cosmos.esa.int/gaia>), processed by the *Gaia* Data Processing and Analysis Consortium (DPAC, <https://www.cosmos.esa.int/web/gaia/dpac/consortium>). Funding for the DPAC has been provided by national institutions, in particular the institutions participating in the *Gaia* Multilateral Agreement. This research has made use of the services of the ESO Science Archive Facility.

*Facility:* SOAR, Gaia

## REFERENCES

- Antognini, J. M. O., & Thompson, T. A. 2016, MNRAS, 456, 4219, doi: [10.1093/mnras/stv2938](https://doi.org/10.1093/mnras/stv2938)
- Brandt, T. D. 2018, ApJS, 239, 31, doi: [10.3847/1538-4365/aaec06](https://doi.org/10.3847/1538-4365/aaec06)
- Bressan, A., Marigo, P., Girardi, L., et al. 2012, MNRAS, 427, 127, doi: [10.1111/j.1365-2966.2012.21948.x](https://doi.org/10.1111/j.1365-2966.2012.21948.x)
- Briceño, C., & Tokovinin, A. 2017, AJ, 154, 195, doi: [10.3847/1538-3881/aa8e9b](https://doi.org/10.3847/1538-3881/aa8e9b)
- Cvetković, Z., & Pavlović, R. 2020, AJ, 160, 48, doi: [10.3847/1538-3881/ab9825](https://doi.org/10.3847/1538-3881/ab9825)
- Dickson-Vandervelde, D. A., Wilson, E. C., & Kastner, J. H. 2021, AJ, 161, 87, doi: [10.3847/1538-3881/abd0fd](https://doi.org/10.3847/1538-3881/abd0fd)
- Duchêne, G., & Kraus, A. 2013, ARA&A, 51, 269, doi: [10.1146/annurev-astro-081710-102602](https://doi.org/10.1146/annurev-astro-081710-102602)
- Dunhill, A. C., Cuadra, J., & Dougados, C. 2015, MNRAS, 448, 3545, doi: [10.1093/mnras/stv284](https://doi.org/10.1093/mnras/stv284)
- Gaia Collaboration, Brown, A. G. A., Vallenari, A., et al. 2021, A&A, 649, A1, doi: [10.1051/0004-6361/202039657](https://doi.org/10.1051/0004-6361/202039657)
- Grady, C. A., Woodgate, B., Torres, C. A. O., et al. 2004, ApJ, 608, 809, doi: [10.1086/420763](https://doi.org/10.1086/420763)
- Guo, D., de Koter, A., Kaper, L., Brown, A. G. A., & de Bruijne, J. H. J. 2021, A&A, 655, A45, doi: [10.1051/0004-6361/202141205](https://doi.org/10.1051/0004-6361/202141205)
- Hartkopf, W. I., Mason, B. D., Barry, D. J., et al. 1993, AJ, 106, 352, doi: [10.1086/116644](https://doi.org/10.1086/116644)
- Herschel, John Frederick William, S. 1847, Results of astronomical observations made during the years 1834, 5, 6, 7, 8, at the Cape of Good Hope; being the completion of a telescopic survey of the whole surface of the visible heavens, commenced in 1825
- Hoogerwerf, R., de Bruijne, J. H. J., & de Zeeuw, P. T. 2000, ApJL, 544, L133, doi: [10.1086/317315](https://doi.org/10.1086/317315)
- Horch, E. P., Casetti-Dinescu, D. I., Camarata, M. A., et al. 2017, AJ, 153, 212, doi: [10.3847/1538-3881/aa6749](https://doi.org/10.3847/1538-3881/aa6749)
- Horch, E. P., Tokovinin, A., Weiss, S. A., et al. 2019, AJ, 157, 56, doi: [10.3847/1538-3881/aaf87e](https://doi.org/10.3847/1538-3881/aaf87e)
- Horch, E. P., Broderick, K. G., Casetti-Dinescu, D. I., et al. 2021, AJ, 161, 295, doi: [10.3847/1538-3881/abf9a8](https://doi.org/10.3847/1538-3881/abf9a8)
- Hwang, H.-C., El-Badry, K., Rix, H.-W., et al. 2022, ApJL, 933, L32, doi: [10.3847/2041-8213/ac7c70](https://doi.org/10.3847/2041-8213/ac7c70)
- Innes, R. 1905, Ann. Cape Obs., 2, Pt. 4
- Lyo, A. R., Lawson, W. A., & Bessell, M. S. 2008, MNRAS, 389, 1461, doi: [10.1111/j.1365-2966.2008.13688.x](https://doi.org/10.1111/j.1365-2966.2008.13688.x)
- Mason, B. D., Wycoff, G. L., Hartkopf, W. I., Douglass, G. G., & Worley, C. E. 2001, AJ, 122, 3466, doi: [10.1086/323920](https://doi.org/10.1086/323920)
- Moe, M., & Di Stefano, R. 2017, ApJS, 230, 15, doi: [10.3847/1538-4365/aa6fb6](https://doi.org/10.3847/1538-4365/aa6fb6)
- Murphy, S. J., Lawson, W. A., & Bessell, M. S. 2013, MNRAS, 435, 1325, doi: [10.1093/mnras/stt1375](https://doi.org/10.1093/mnras/stt1375)
- Reipurth, B. 2000, AJ, 120, 3177, doi: [10.1086/316865](https://doi.org/10.1086/316865)
- Tokovinin, A. 2017, ORBIT3: Orbits of Triple Stars, Zenodo, doi: [10.5281/zenodo.321854](https://doi.org/10.5281/zenodo.321854)
- . 2018a, AJ, 155, 160, doi: [10.3847/1538-3881/aab102](https://doi.org/10.3847/1538-3881/aab102)
- . 2018b, PASP, 130, 035002, doi: [10.1088/1538-3873/aaa7d9](https://doi.org/10.1088/1538-3873/aaa7d9)
- . 2018c, ApJS, 235, 6, doi: [10.3847/1538-4365/aaa1a5](https://doi.org/10.3847/1538-4365/aaa1a5)
- . 2020, Astronomy Letters, 46, 612, doi: [10.1134/S1063773720090078](https://doi.org/10.1134/S1063773720090078)
- . 2021a, Universe, 7, 352, doi: [10.3390/universe7090352](https://doi.org/10.3390/universe7090352)
- . 2021b, AJ, 161, 144, doi: [10.3847/1538-3881/abda42](https://doi.org/10.3847/1538-3881/abda42)
- Tokovinin, A., Fischer, D. A., Bonati, M., et al. 2013, PASP, 125, 1336, doi: [10.1086/674012](https://doi.org/10.1086/674012)
- Tokovinin, A., & Latham, D. W. 2017, ApJ, 838, 54, doi: [10.3847/1538-4357/aa6331](https://doi.org/10.3847/1538-4357/aa6331)
- . 2020, AJ, 160, 251, doi: [10.3847/1538-3881/abba4](https://doi.org/10.3847/1538-3881/abba4)
- Tokovinin, A., Mason, B. D., & Hartkopf, W. I. 2010, AJ, 139, 743, doi: [10.1088/0004-6256/139/2/743](https://doi.org/10.1088/0004-6256/139/2/743)
- Tokovinin, A., Mason, B. D., Hartkopf, W. I., Mendez, R. A., & Horch, E. P. 2016, AJ, 151, 153, doi: [10.3847/0004-6256/151/6/153](https://doi.org/10.3847/0004-6256/151/6/153)
- Tokovinin, A., Mason, B. D., Mendez, R. A., & Costa, E. 2022, AJ, 164, 58, doi: [10.3847/1538-3881/ac78e7](https://doi.org/10.3847/1538-3881/ac78e7)
- Tokovinin, A., & Moe, M. 2020, MNRAS, 491, 5158, doi: [10.1093/mnras/stz3299](https://doi.org/10.1093/mnras/stz3299)
- van Leeuwen, F. 2007, A&A, 474, 653, doi: [10.1051/0004-6361:20078357](https://doi.org/10.1051/0004-6361:20078357)